ISSN 0022-4766, Journal of Structural Chemistry, 2019, Vol. 60, No. 12, pp. 1868-1876. © Pleiades Publishing, Ltd., 2019.
Russian Text © The Author(s), 2019, published in Zhurnal Strukturnoi Khimii, 2019, Vol. 60, No. 12, pp. 1949-1958.

CRYSTAL AND ELECTRONIC STRUCTURES OF ALLUAUDITE-TYPE DOUBLE MOLYBDATES OF SCANDIUM AND INDIUM

D. V. Suetin[1], Ya. V. Baklanova[1]*, N. I. Medvedeva[1], A. A. Savina[2,3], E. G. Khaykina[3], E. D. Pletneva[4], and T. A. Denisova[1]

Double molybdates of indium and scandium with alluaudite structure are prepared by the solid-phase synthesis method. The crystal structure of the indium containing compound is refined and optical characteristics of $Na_5R(MoO_4)_4$ (R = Sc, In) are determined. Electronic structures of $Na_5R(MoO_4)_4$ (R = Sc, In) molybdates are studied within the ab initio method taking account of Na/Sc(In) positional disordering. Calculations of the imaginary part of dielectric function predict the optical gap of ~3.8 eV, in accordance with absorption spectroscopy data. It is established that formation energy of sodium vacancies strongly depends on sodium position and Sc(In) concentration. As a result, various diffusion mechanisms may be activated in alluaudite-type compounds with high and low contents of metal R.

DOI: 10.1134/S0022476619120023

Keywords: double molybdate, indium, scandium, solid-phase synthesis, crystalline structure, Rietveld method, electronic structure, ab initio calculations.

INTRODUCTION

Rapid progress in the production of electrochemical power sources gains increasing interest to the search and development of novel complex oxide solid electrolytes having open framework structures and containing mobile ions inside their channels. Among known framework materials with high ionic conductivity, compounds with alluaudite structure (Na, Ca)(Fe, Mn, Mg)$(PO_4)_3$ hold a special place [1]. Sulfates and phosphates of polyvalent elements with such structure are well studied; due to their structural features, they exhibit not only high conductivity (ionic and/or electronic) but also some properties that make these materials suitable for the use in Li- and Na-ion batteries [2-4]. Besides phosphates and sulfates, there are alluaudite-type arsenates [5], vanadates [6], as well as sodium molybdates with di- and trivalent cations whose high ionic conductivities (~10^{-4}-10^{-3} S/cm at 400-500 °C) allow them to be used as solid electrolytes [7-11]. Isostructural compounds $Na_5R(MoO_4)_4$ (R = In, Sc) are typical representatives of molybdates with alluaudite structure [7]. Their crystal structure was determined from X-ray data on the example of a scandium compound by Klevtsova et al. [12] and refined in

[1]Institute of Solid State Chemistry, Ural Branch, Russian Academy of Sciences, Ekaterinburg, Russia; *baklanovay@ihim.uran.ru. [2]Skolkovo Institute of Science and Technology, Moscow, Russia. [3]The Baikal Institute of Nature Management, Siberian Branch, Russian Academy of Sciences, Ulan-Ude, Russia. [4]Ural Federal University, Ekaterinburg, Russia. Original article submitted March 26, 2019; revised July 1, 2019; accepted July 8, 2019.

our work by the Rietveld method for a polycrystalline sample [11]. The structure consists of polyhedra layers formed by pairs of sodium and scandium octahedra joined along their edges and linked at their vertices to bridging MoO_4 tetrahedra [11, 12]. In turn, these layers form a three-dimensional framework with sodium cations inside its cavities. Such crystal structure implies a presence of one-dimensional channels for the migration of sodium ions. However, a more complex mechanism of ion diffusion can be assumed in alluaudite-type compounds due to complex relative arrangement of sodium positions and their partial and mixed occupancy. This works presents an experimental and theoretical study of crystal and electron structures of alluaudite-type sodium-containing complex molybdenum oxides $Na_5R(MoO_4)_4$ (R = Sc, In).

EXPERIMENTAL

Double molybdates $Na_5R(MoO_4)_4$ (R = Sc, In) were obtained according to the standard ceramic technology by annealing stoichiometric amounts of Na_2MoO_4 and $R_2(MoO_4)_3$ molybdates at 550-570 °C for 80 h accompanied by repeated grinding every 15 h for better homogenization. Anhydrous Na_2MoO_4 was obtained by the calcination of the corresponding crystal hydrate (reagent-grade) at 550-600 °C. Indium and scandium molybdates $R_2(MoO_4)_3$ were prepared at 450-700 °C for 80 h by the calcination of stoichiometric mixtures of corresponding oxides with molybdenum trioxide (all reagent-grade substances).

X-ray powder diffraction (XRD) of prepared compounds and the refinement of their crystal structures were carried out using the data obtained in a Huber 670 high-resolution Guinier camera (transmission geometry, linear PSD detector, Ge(111) monochromator, CoK_{α_1} radiation with λ = 1.78892 Å, 2θ-range is 5-100°). The phase analysis was conducted using ICDD PDF2 and PDF4 databases. The structure of $Na_5In(MoO_4)_4$ was refined with the Rietveld full-profile method using the JANA2006 package. The diffuse reflectance spectra were recorded in the wavelength range of 200-800 nm on a Shimadzu UV-3600 spectrophotometer equipped with a ISR 3100 unit with an integrating sphere. $BaSO_4$ (99.9%) was used as the reference compound.

Calculations of $Na_x(Sc,In)_y(MoO_4)_4$ were performed by the projector augmented-wave (PAW) method using the Vienna Ab initio Simulation Package (VASP) [13, 14] and Perdew–Burke–Ernzerhof (PBE) generalized gradient approximation for the exchange-correlation potential [15]. The Brillouin zone was integrated over a 2×2×4 k-grid [16], the kinetic energy cut-off was 400 eV. Simulation of disordered structures is a big problem, since density functional methods are designed for ordered structures where each position is occupied by a single atom. The existing approaches to disordered structures do not reliably predict optimized geometries and cannot be used to calculate characteristics depending on local charge density distribution such as electric field gradients on the nuclei. The electronic structure of partially disordered molybdates was studied using an 80-atomic ordered elementary cell with various Sc(In)/Na ratios in the R/Na position. Atomic positions were optimized by the gradient method with a force convergence of 0.01 eV/Å for fixed experimental lattice parameters.

RESULTS AND DISCUSSION

Crystal structure. As noted above, $Na_5R(MoO_4)_4$ (R = Sc, In) compounds are isostructural. Their crystal structure was defined and refined on the example of R = Sc (space group $C2/c$, a = 12.88737(7) Å, b = 13.89612(7) Å, c = 7.24874(4) Å, β = 113.0269(5)°, Z = 3 [11]). In the present work, we attempted to refine the $Na_5In(MoO_4)_4$ crystal structure with the Rietveld method using powder XRD data. The coordinates of basis atoms in the structure of the scandium analog were used as initial parameters [11]. The conditions of X-ray experiments and main refinement data are summarized in Table 1; coordinates of basis atoms, thermal parameters, and main interatomic distances are listed in Tables 2 and 3. After the refinement of all parameters, the chosen model demonstrated good agreement between experimental and calculated XRD patterns (Fig. 1). The crystallographic data were deposited with the Cambridge Crystallographic Data Centre (CSD number 1903682).

TABLE 1. Experimental Conditions and Structure Refinements of $Na_5In(MoO_4)_4$

Parameter	Value
Temperature, K	297
2θ range, deg	5-100
Scanning step size, 2θ, deg	0.005
I_{max}	7987
Number of points	19000
Number of refined parameters	58
d_{calc}, g/cm^3	3.6096
Space group; No.	*C*2/*c*; 15
Z	3
Unit cell parameters: *a*, *b*, *c*, Å	12.88220(7), 13.90022(8), 7.27853(4)
β, deg	112.9670(4)
V, Å^3	1200.018(12)
wR_p / R_p,%	4.86 / 3.51
$R(F^2)$,%	3.50
χ^2	1.39
Largest diff. peak / hole	0.94 / –1.03

TABLE 2. Atomic Coordinates and Isotropic Thermal Parameters for $Na_5In(MoO_4)_4$

Atom	Position	Occupancy	*x*/*a*	*y*/*b*	*z*/*c*	U_{iso}*/U_{eq}
Mo1	4*e*	1	0	0.79266(11)	0.25	0.0049(6)
Mo2	8*f*	1	0.22608(9)	0.61160(8)	0.12358(16)	0.0045(4)
Na1	4*e*	1	0	0.2310(5)	0.25	0.013(2)
Na2	4*a*	1	0	0	0	0.088(3)
Na3	4*e*	0.5	0	0.5266(12)	0.25	0.088(3)
Na / In	8*f*	0.625 / 0.375	0.2912(2)	0.84063(10)	0.3778(3)	0.0093(7)
O1	8*f*	1	0.0333(5)	0.7133(5)	0.4566(9)	0.0220(19)
O2	8*f*	1	0.1045(5)	0.8739(4)	0.2536(10)	0.0220(19)
O3	8*f*	1	0.2144(5)	0.6821(4)	0.3080(9)	0.0085(12)
O4	8*f*	1	0.1575(4)	0.5044(5)	0.0970(8)	0.0085(12)
O5	8*f*	1	0.3628(5)	0.5849(4)	0.1786(8)	0.0085(12)
O6	8*f*	1	0.1572(5)	0.6714(4)	–0.1292(9)	0.0085(12)

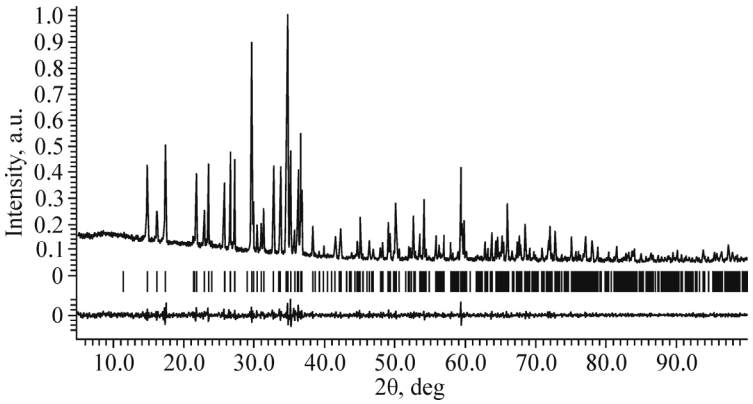

Fig. 1. Experimental, calculated, and difference XRD diffractograms and Bragg reflections (vertical bars) for $Na_5In(MoO_4)_4$.

TABLE 3. Main Interatomic Distances for $Na_5In(MoO_4)_4$

Mo1 tetrahedron		Mo2 tetrahedron	
Mo1–O1	1.777(7)×2	Mo2–O3	1.715(7)
Mo1–O2	1.749(6)×2	Mo2–O4	1.704(7)
⟨Mo1–O⟩	1.763	Mo2–O4	1.688(6)
		Mo2–O6	1.894(6)
		⟨Mo2–O⟩	1.750
Na1 octahedron		Na2 polyhedron	
Na1–O6	2.307(7)×2	Na2–O5	2.600(5)×2
Na1–O1	2.461(8)×2	Na2–O2	2.520(5)×2
Na1–O5	2.607(8)×2	Na2–O5′	2.828(5)×2
⟨Na1–O⟩	2.458	Na2–O2′	2.601(5)×2
		⟨Na2–O⟩	2.637
Na3 polyhedron		Na/In octahedron	
Na3–O4	2.585(5)×2	Na/In–O1	2.236(6)
Na3–O4′	2.585(5)×2	Na/In–O2	2.263(6)
Na3–O6	2.686(6)×2	Na/In–O3	2.388(6)
Na3–O3	2.945(1)×2	Na/In–O4	2.357(7)
⟨Na3–O⟩	2.646	Na/In–O6	2.164(8)
		Na/In–O3′	2.388(6)
		⟨Na/In–O⟩	2.299

In the structure of $Na_5In(MoO_4)_4$, molybdenum atoms are in tetrahedral coordination, indium atoms occupy their positions together with sodium atoms and occur in octahedral coordination. The remaining Na atoms occupy three crystallographically non-equivalent positions with different oxygen environments (Table 3), so that Na3 positions are half-occupied (Table 2). The pairs of $(In,Na)O_6$ and $Na1O_6$ octahedra joined along their edges are linked at common vertices to MoO_4 tetrahedra to form layers similar to polyhedral layers in the alluaudite structure [1]. The layers are linked by bridging MoO_4 tetrahedra into a three-dimensional framework containing Na2 and Na3 cations inside its cavities. $Na2O_8$ and $Na3O_8$ polyhedra form two large hexagonal conduction channels oriented along the *c* axis and interacting with each other through $Na1O_6$ octahedra (Fig. 2). Thus, the crystal structure indicates that $Na_5R(MoO_4)_4$ (R = Sc, In) compounds may exhibit two-dimensional conductivity and that the diffusion of sodium ions can proceed not only directly through Na2 and Na3 channels along the *c* axis but also with the participation of an intermediate Na1 position.

Optical characteristics. Fig. 3 shows the diffuse reflectance spectra of $Na_5R(MoO_4)_4$ (R = Sc, In) recorded at 250-750 nm. The compounds are transparent and have no absorption bands in this wavelength region. The absorption spectra were obtained from the diffuse reflectance spectrum using the modified Kubelka–Munk function [17]. The band gap E_g was determined by extrapolating the linear part of the $[F(R_\infty)\cdot hv]^n$ graph as a function of hv, where n is a constant depending on the type of the interband transition. However, the intensity of forbidden transitions is low and their contribution to the experimental dependence of diffuse reflection on the wavelength is insignificant in polycrystalline samples, and indirect transitions are typical of non-crystalline materials [18]. Also, the longest straight-lined sections along the *x*-axis are observed in $[F(R_\infty)hv]^2 = f(hv)$ (n = 1/2) dependences and indicate that the absorption edge of considered molybdates is formed by direct allowed transitions. Thus, the E_g values for $Na_5Sc(MoO_4)_4$ and $Na_5In(MoO_4)_4$ determined from the fundamental absorption edge in the case of direct allowed transitions are 4.2 eV and 3.9 eV, respectively (Fig. 3, inset).

Electronic structure. Electronic properties of molybdates as functions of Sc(In) content were analyzed by considering three model compounds whose sublattices formed by Na atoms in *R*/Na positions had different occupancies by Sc(In) atoms. In the first case, the *R*/Na position is filled only by Na atoms ($Na_{6.67}(MoO_4)_4$); in the second case, Na and Sc(In)

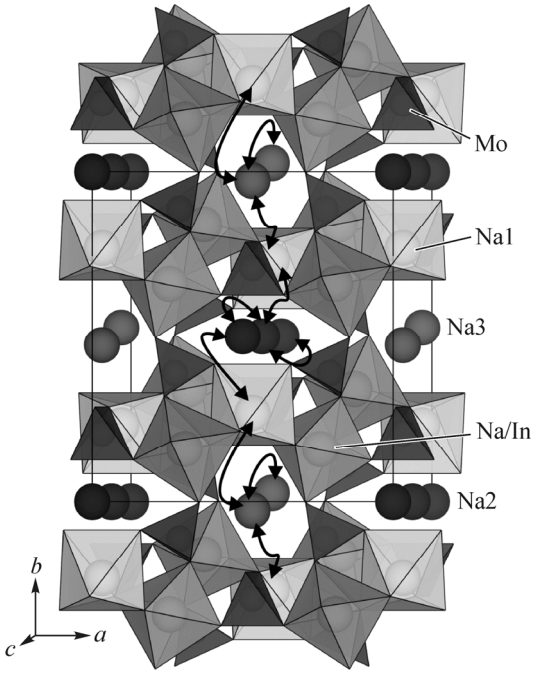

Fig. 2. $Na_5In(MoO_4)_4$ structure along [001] directions: diffusion path of Na^+ ions are shown by arrows.

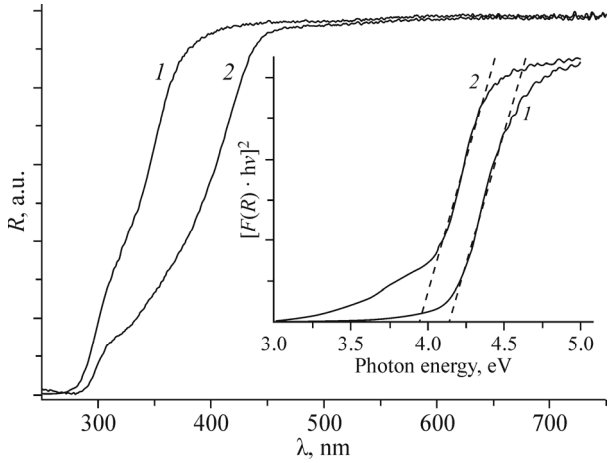

Fig. 3. Diffuse reflectance spectra of $Na_5Sc(MoO_4)_4$ (*1*) and $Na_5In(MoO_4)_4$ (*2*) compounds in the range of 250-750 nm. Inset: spectra of $Na_5Sc(MoO_4)_4$ (*1*) and $Na_5In(MoO_4)_4$ (*2*) written in the $[F(R_\infty)h\nu]^2 = f(h\nu)$ form in the assumption of direct allowed transitions.

atoms were present in molybdates in equal ratios in *R*/Na positions ($Na_{5.33}(Sc,In)_{1.33}(MoO_4)_4$); and in the third case, the corresponding positions were occupied only by Sc(In) atoms ($Na_4(Sc,In)_{2.67}(MoO_4)_4$).

Fig. 4*a* shows calculated total and partial densities of states (TDOS and PDOS, respectively) for $Na_{5.33}Sc_{1.33}(MoO_4)_4$, which is most close in composition to $Na_5Sc(MoO_4)_4$. As is seen, the valence band is divided by a pseudogap into two subbands from –4 eV to –2.5 eV and from –2.5 eV to 0 eV. The low-energy band is composed of O2*p*, Mo4*d*, and Sc3*d* valence states, and the upper part of the valence band consists mainly of O2*p* and Sc3*d* states. The contribution of Na2*s*,2*p* states to the TDOS is much lower in the whole energy range from –4 eV to 6 eV. The PDOSs of non-equivalent sodium atoms differ insignificantly, the most intense peaks correspond to sodium states in *R*/Na positions, and the

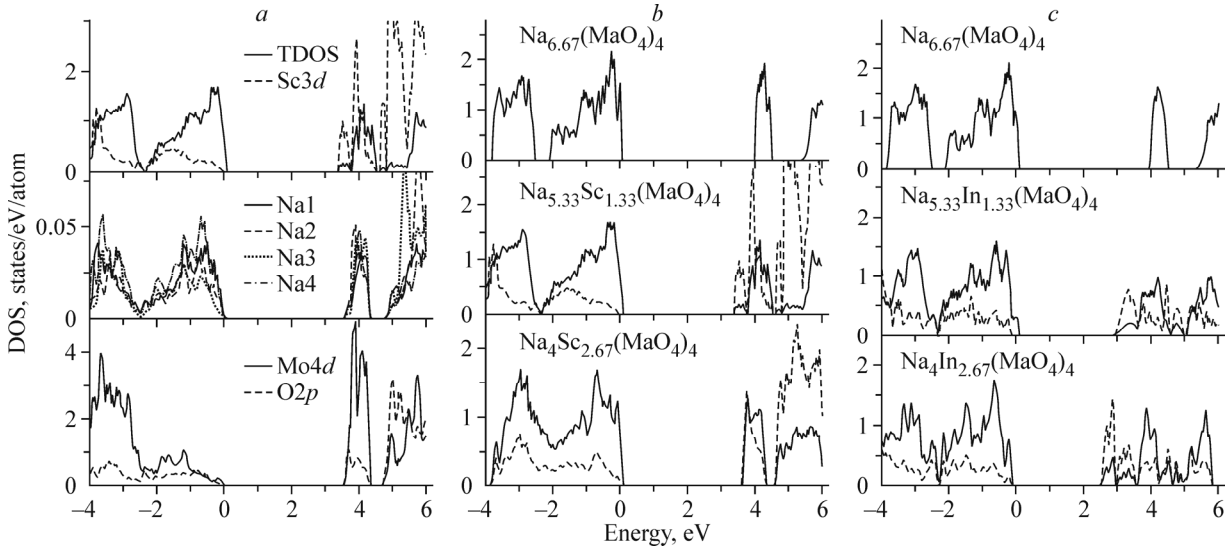

Fig. 4. Total and partial densities of states for $Na_{5.33}Sc_{1.33}(MoO_4)_4$ (*a*), $Na_xSc_y(MoO_4)_4$ (*b*), and $Na_xIn_y(MoO_4)_4$ (*c*).

lowest-intensity peaks correspond to Na3 states. This molybdate is an insulator with a band gap $E_g \sim 3.4$ eV. The bottom of the conduction band is composed mainly by scandium and molybdenum *d*-states. Mo4*d* states provide a significant contribution to the bottom of the conduction band, and Sc3*d* states are predominant in the vicinity of 5 eV. It should be noted that Mo4*d*, O2*p*, and Na3*s*,3*p* vacant states form two subbands separated by a band gap of ~0.3 eV, while Sc3*d* states exhibit no such splitting.

Let us analyze the changes in the total and partial densities of states in molybdate depending on the occupancy of *R*/Na positions by Sc(In) atoms. According to the calculations of model structures, the E_g value is decreased as the Sc(In) concentration increases. This decrease is monotonic for the system with indium: 3.94 eV, 2.90 eV, and 2.16 eV for $Na_{6.67}(MoO_4)_4$, $Na_{5.33}In_{1.33}(MoO_4)_4$, and $Na_4In_{2.67}(MoO_4)_4$, respectively. For scandium molybdate, the band gap varies from 3.98 eV to 3.48 eV and 3.59 eV in this series of compositions. Since scandium and indium states determine the main features of the electron spectrum near the conduction band bottom (Fig. 4), the presence of these atoms substantially decreases the band gap as compared to $Na_{6.67}(MoO_4)_4$ which contains only Na atoms in *R*/Na positions. For $Na_{5.33}Sc(In)_{1.33}(MoO_4)_4$, which is most close in composition to $Na_5R(MoO_4)_4$, the E_g value is about 3.4 eV and 2.9 eV for *R* = Sc and In, respectively.

The above unit cells are not electrically neutral. We also calculated ordered unit cells $Na_{15}Sc(In)_3(MoO_4)_{12}$ containing three scandium (indium) atoms and two vacancies in the Na3 position. These supercells are electrically neutral and correspond exactly to the experimental compound $Na_5R(MoO_4)_4$. Total and partial densities of states are shown in Fig. 5. For

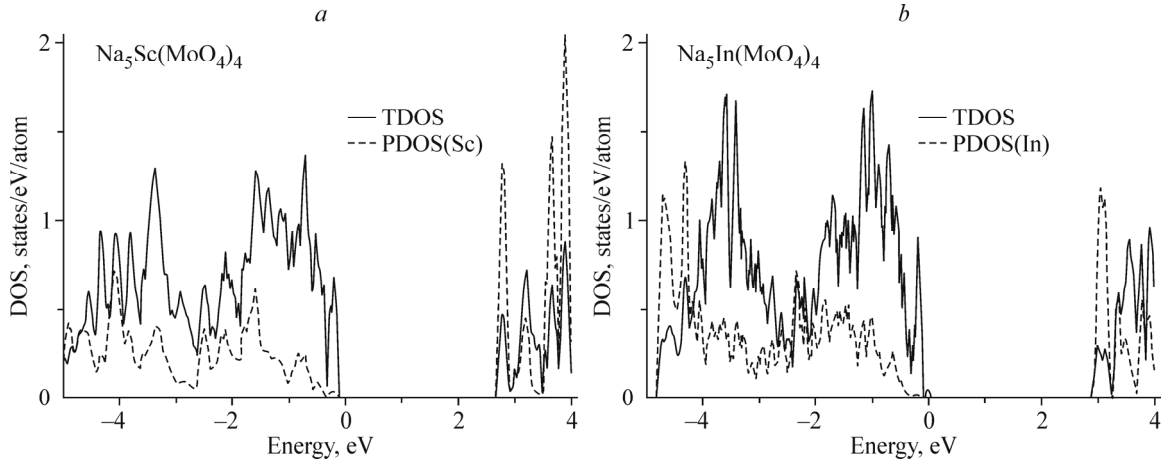

Fig. 5. Total and partial densities of states for $Na_5Sc(MoO_4)_4$ (*a*) and $Na_5In(MoO_4)_4$ (*b*) corresponding to electrically neutral compositions.

this compound, the band gap obtained from the density of states is 2.6 eV and 2.8 eV for scandium and indium molybdate, respectively. Thus, taking into account charge compensation, the E_g value should depend weakly on the type of the trivalent atom *R*. Note that the calculated band gaps correspond to the structures with ordered scandium (indium) positions and vacancies which cause additional peaks near the bottom of the conduction band.

To interpret optical properties, we calculated the imaginary part of dielectric permittivity $\varepsilon_2(\omega)$ in a wide range of absorption energies for $Na_6R_{0.67}(MoO_4)_4$ and $Na_{5.33}R_{1.33}(MoO_4)_4$ compositions containing two and four *R* atoms, respectively (Fig. 6). The $\varepsilon_2(\omega)$ spectrum allows analyzing energies and intensities of major transitions. For transparent materials, the imaginary part of dielectric function determines the optical absorption coefficient. The peaks in the spectra of all compounds occur at ~4.3–4.5 eV, and the optical absorption edge occurs at ~3 eV. As the concentration of *R* increases, the intensity of the main peak varies for scandium and indium molybdates, but its position does not change significantly. The optical gap calculated from the imaginary part of dielectric function (~3.8 eV) agrees well with experimental values for these molybdates.

Effective charges on sodium atoms and atomic volumes were calculated within the Bader approach [19]. The approach assumes that the maximum charge density is localized on nuclei, and the atoms are separated by the regions of minimal charge density. An atom is defined as a region of space limited by the surfaces having zero flux in the gradient of the electron density $\nabla\rho = 0$.

Approximately equal Na charges (close to the ionic charge +0.9) were obtained for all non-equivalent positions and for all $Na_xSc_y(MoO_4)_4$ and $Na_xIn_y(MoO_4)_4$ compositions (Table 4). Atomic volume of sodium, which characterizes the spatial

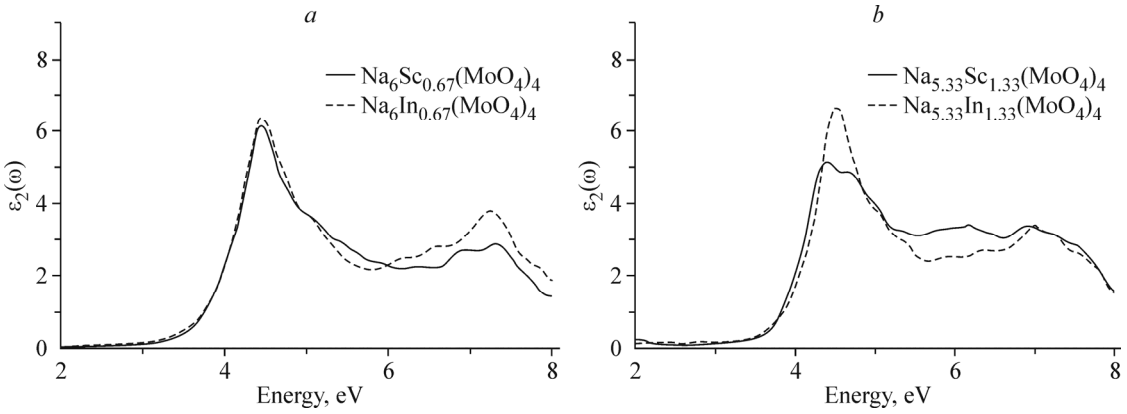

Fig. 6. Imaginary part of dielectric function calculated for $Na_6R_{0.67}(MoO_4)_4$ and $Na_{5.33}R_{1.33}(MoO_4)_4$ (*R* = Sc (*1*); In (*2*)).

TABLE 4. Effective Charges (e) on Sodium Atoms and Their Atomic Volumes (Å^3) in $Na_xR_y(MoO_4)_4$ for the Model Unit Cell with Missing *R* Atoms (*y* = 0) and with 8 *R* Atoms (*y* = 2.66)

Position	$Na_xSc_y(MoO_4)_4$			$Na_xIn_y(MoO_4)_4$		
	y = 0	*y* = 2.66	*y* = 1*	*y* = 0	*y* = 2.66	*y* = 1*
Na1	+0.89 (8.45)**	+0.89 (8.84)	+0.90 (8.58)	+0.89 (8.47)	+0.89 (8.38)	+0.89 (8.51)
Na2	+0.91 (9.74)	+0.90 (9.75)	+0.90 (9.77)	+0.91 (9.76)	+0.90 (9.65)	+0.91 (9.72)
Na3	+0.91 (9.73)	+0.90 (10.66)	+0.91 (10.32)	+0.90 (9.78)	+0.90 (9.67)	+0.91 (9.86)
R/Na	+0.89 (7.73)	–	+0.89 (8.06)	+0.89 (7.72)	–	+0.89 (7.96)

* Average values are given for $Na_5R(MoO_4)_4$ (*y* = 1).

** Atomic volumes are given in parentheses.

TABLE 5. Formation Energy of Vacancies E_{form} (eV) for Different Sodium Positionsin $Na_xR_y(MoO_4)_4$ (R = Sc, In)

Position	$Na_xSc_y(MoO_4)_4$		$Na_xIn_y(MoO_4)_4$	
	$y = 0$	$y = 2.66$	$y = 0$	$y = 2.66$
Na1	4.98	1.21	4.97	1.18
Na2	4.69	1.09	4.70	0.85
Na3	4.71	0.64	4.68	0.57
R/Na	5.07	–	5.02	–

charge distribution, undergoes more substantial changes. The calculated volume shows the most compact charge distribution for Na atoms in the position of the *R*/Na metal; the distribution increases in the presence of *R* atoms but almost does not depend on its type. In the absence of scandium/indium ($y = 0$), Na2 and Na3 atoms have equal volumes for both systems, and the volume of the Na1 atom is substantially smaller than the Na2 and Na3 volumes. The presence of a trivalent atom leads to the redistribution of charge density, which is essential only for Na3 atoms in scandium molybdate and does not occur in indium molybdate. The increased atomic volume of Na3 should promote the diffusion of Na atoms along the linear channel in the direction of the *c* axis.

Formation energy of sodium vacancies. The diffusion of sodium ions proceeds according to the vacancy mechanism; therefore, it is important to estimate the vacancy formation energy in different non-equivalent sodium positions. We calculated two extreme occupancies of *R*/Na positions when scandium/indium atoms are absent ($y = 0$) and when they completely fill this position ($y = 2.66$) in $Na_xR_y(MoO_4)_4$ to make some conclusions concerning the influence of scandium/indium local distribution on the vacancy formation energy. To model a single vacancy, the sodium atom was removed from Na1, Na2, Na3 or *R* positions, and all atomic coordinates were optimized to equilibrium positions. The vacancy formation energy, E_{form}, was estimated as a difference between total energies of ideal and defective unit cells taking account of sodium chemical potential μ_{Na}. Since the main goal was to find E_{form} for various Na positions, the μ_{Na} value was taken equal to the total energy of metallic body-centered cubic lattice of Na, while the effects of pressure and temperature were not considered. According to the calculations (Table 5), when *R*/Na positions are filled with sodium atoms, Na2 and Na3 positions have equal vacancy formation energies, which are ~0.3 eV lower than those in Na1 and *R*/Na. The E_{form} value is the largest for the vacancies in the sodium *R*/Na position.

Much smaller formation energies of sodium vacancies were obtained for the unit cell with all eight *R*/Na positions filled by scandium/indium atoms. In this case, the lowest and the highest formation energies correspond to Na3 and Na1 position, respectively. Thus, the vacancy formation energy in $Na_xR_y(MoO_4)_4$ substantially differs for various non-equivalent sodium positions and depends on the concentration of trivalent metal *R*. According to our calculations, the presence of scandium/indium leads to the formation of vacancies in the Na3 position, and high concentration of Na3 vacancies contributes to high ionic conductivity with the participation of this position. However, the regions with low concentrations of the trivalent metal can exhibit diffusion of Na1 ions, since they have the same binding energy as sodium and other atoms. Moreover, Na1→Na3 transitions were determined by the difference between the vacancy formation energies for these positions [2, 11]. The threshold of this transition (~0.3 eV for $y = 0$) is two times lower in the region distant from metal *R* than in the region of high concentration of metal *R* (~0.6 eV for $y = 2.66$), Table 5. Such two-dimensional diffusion is an additional source of mobile ions in Na3–Na3 and Na2–Na2 one-dimensional channels along the *c* axis.

CONCLUSIONS

In this work, double molybdates with alluaudite structure $Na_5R(MoO_4)_4$ (R = Sc, In) were obtained using the standard ceramic technique, the crystal structure was refined for R = In and optical characteristics were determined. The three-dimensional framework of alluaudite-type compounds favors two-dimensional diffusion of sodium ions through Na2

and Na3 channels along the *c* axis, as well as the diffusion with the participation of Na1 positions. The electronic structure of scandium and indium molybdates $Na_5R(MoO_4)_4$ (R = Sc, In) was studied using the ab initio method. These molybdates were shown to be insulators, and the optical gap of ~3.8 eV obtained from the imaginary part of dielectric function agrees well with experimental values for these molybdates. The formation energy of sodium vacancies depends on their positions and on the metal concentration. High concentration of scandium/indium substantially diminishes the formation energy of sodium vacancies, which should contribute to the ionic diffusion in the vicinity of these atoms. The regions of low concentrations of the R metal may exhibit diffusion of Na1 ions. Such diffusion is an additional source of mobile ions in one-dimensional channels and may lead to 2D conductivity.

FUNDING

This work was supported by the RSF project No. 18-12-00395.

CONFLICT OF INTERESTS

The authors declare that they have no conflict of interests.

REFERENCES

1. P. B. Moore. *Am. Mineral.*, **1971**, *56*, 1955.
2. P. Barpanda, G. Oyama, S. Nishimura, S.-C. Chung, and A. Yamada. *Nat. Commun.*, **2014**, *5*, 4358.
3. C. Masquelier and L. Croguennec. *Chem. Rev.*, **2013**, *113*, 6552.
4. J. Lu and A. Yamada. *ChemElectroChem*, **2016**, *3*, 902.
5. S. K. Filatov, L. P. Vergasova, M. G. Gorskaya, S. V. Krivovichev, P. C. Burns, and V. V. Ananiev. *Can. Mineral.*, **2001**, *39*, 1115.
6. E. Benhsina, A. Assani, M. Saadi, L. and El Ammari. *Acta Crystallogr.*, **2016**, *E72*, 220–222.
7. Yu. A. Velikodnyj and V. K. Trunov. *Neorg. Mat.*, **1974**, *7*, 1290.
8. A. A. Savina, S. F. Solodovnikov, D. A. Belov, Z. A. Solodovnikova, S. Yu. Stefanovich, B. I. Lazoryak, and E. G. Khaikina. *New J. Chem.*, **2017**, *41*, 5450.
9. J. Gao, P. Zhao, and K. Feng. *Chem. Mater.*, **2017**, *29*, 940.
10. S. F. Solodovnikov, Z. A. Solodovnikova, E. S. Zolotova, V. N. Yudin, O. A. Gulyaeva, Y. L. Tushinova, and B. M. Kuchumov. *J. Solid State Chem.*, **2017**, *253*, 121.
11. N. I. Medvedeva, A. L. Buzlukov, A. V. Skachkov, A. A. Savina, V. A. Morozov, Y. V. Baklanova, I. E. Animitsa, E. G. Khaikina, T. A. Denisova, and S. F. Solodovnikov. *J. Phys. Chem. C*, **2019**, *123*, 4729.
12. R. F. Klevtsova, L. P. Kozeeva, and P. V. Klevtsov. *Kristallografiya*, **1975**, *20*, 925.
13. G. Kresse and J. Furthmuller. *Phys. Rev. B*, **1996**, *54*, 11169.
14. G. Kresse and J. Hafner. *J. Phys. - Condens. Mat.*, **1996**, *6*, 8245.
15. J. P. Perdew, K. Burke, and M. Ernzerhof. *Phys. Rev. Lett.*, **1996**, *77*, 3865.
16. H. J. Monkhorst and J. D. Pack. *Phys. Rev. B*, **1976**, *13*, 5188.
17. M. L. Myrick, M. N. Simcock, M. Baranowski, H. Brooke, S. L. Morgan, and J. N. McCutcheon. *Appl. Spectrosc. Rev.*, **2011**, *46*, 140.
18. J. Tauc. *Mater. Res. Bull.*, **1968**, *3*, 37.
19. R. Bader. Atoms in Molecules: A Quantum Theory. Oxford University Press: UK, Oxford, **1990**.